

Scanning Tunneling Microscopy Study of DNA–Chromophore Motif on Solid Surfaces

Wenli Deng,^{*,†} Zhanwen Xiao,[†] Wei Wang,[‡] and Alexander D. Q. Li^{*,‡}*College of Materials Science and Engineering, South China University of Technology, Guangzhou 510640, China, and Department of Chemistry, Washington State University, Pullman, Washington 99164**Received: January 31, 2007; In Final Form: March 22, 2007*

We focus our studies on DNA–chromophore motif on surfaces using samples prepared by the synthetic methods described by Wang and Li in a recent publication (*J. Am. Chem. Soc.* **2003**, *125*, 5248–5249). Scanning tunneling microscope (STM) was used to investigate the DNA–chromophore hybrids adsorbed on Au(111) and highly oriented pyrolytic graphite (HOPG) surfaces at room temperature in air. Experiments found that the DNA–chromophore hybrid molecules easily formed multimolecule aggregations on gold surface. On HOPG surfaces, however, DNA–chromophore hybrids were usually adsorbed as single molecules. STM images further showed DNA–chromophore hybrids adsorbed on Au(111) surfaces existed in the form of single molecule, dimer, trimer, tetramer, etc. The occurrence of molecular aggregations indicates that molecular interactions are comparable or stronger than molecule–substrate interactions; such weak interactions control the geometrical sizes and topographical shapes of the self-assembled DNA–chromophore hybrids on surfaces.

1. Introduction

Scanning tunneling microscope (STM)¹ has been a powerful tool to image DNA molecules on conductive substrates.² Investigations in solution have established that DNA can transport charges over significant distance.³ The results differ depending upon the nature of the DNA and its sequence, but all emphasize the charge transport properties of duplex DNA. In conductivity measurements, where DNA molecules are located between two electrodes, controversy results have been reported, DNA as ohmic conductor,⁴ semiconductor,⁵ or superconductor.⁶ These measurements, however, lack rigorous considerations of the DNA structure and flexibility, both of which vary significantly with counterion condensation and solvent content. Disruption of the duplex structure or metal–molecules contacts may lead to loss of conductivity.^{7,8} To probe the electronic properties of DNA in a metal–molecule–metal assembly under physiological conditions, Barton and co-worker have investigated thiol-modified DNA films on gold surfaces using *in situ* STM and they have shown the bias and mismatch dependence.⁹

Molecular self-assembly is a superior way to construct molecular three-dimensional architectures and DNA is an ideal material for fabrication of rigid nanostructures because its assembly can be controlled by base-pairing¹⁰ and can be programmed with simple executions. General strategies for the preparation of two-dimensional periodic structures involve a hierarchy of interactions in which pre-assembled building blocks are linked by multiple weak interactions to form an array,^{11–13} but three-dimensional construction has not been well developed. However, DNA polyhedral nanostructures such as a cubes¹⁴ and truncated and regular octahedra,^{15,16} have been made, each using a different synthetic strategy. Tris寡onucleotidyls have also been described to form tetrahedra,¹⁷ in which three oligonucleotides have been connected by a trifunctional linker.¹⁸ Turberfield

and co-workers have synthesized a series of DNA tetrahedra that have been designed to self-assemble in a single step within only a few seconds,¹⁹ and demonstrated the versatility of DNA-based building blocks for three-dimensional nanofabrication by assembling nanosized tetrahedra using programmable DNA linkers.

DNA has been used to functionalize nanoparticles,^{20–22} proteins,²³ and fluorescent dyes^{24–26} as probes and nanowires. Li and co-workers have developed methods for efficient incorporation of multiple optically active chromophores into the backbone of DNA for folding studies.²⁷ The successful strategy is to insert π -conjugated structures into DNA using asymmetric building blocks with one end activated and the other end protected. Their coupling chemistry is compatible with automated DNA syntheses.²⁸ Using this strategy, they have created a motif of alternating optically active chromophores and foldable DNA sequences of 5'-DNA-(TEG-Chr-TEG-ssDNA)_n-TEG-Chr-TEG-DNA-3', where TEG is tetraethylene glycol and Chr is the perylene tetracarboxylic diimide chromophore. The ssDNA are based on NF- κ B DNA binding site and it has a sequence of 5'-ATC-CGG-AGT-CAG-CCG-GAT-3'.²⁷ Using gel electrophoresis, these hybrid sequences have been purified into single molecular weight polymers corresponding to chromophoric dimers, trimers, tetramers, and pentamers linked via ssDNAs. In this paper, we have further investigated the DNA–chromophore hybrids on Au(111) and highly oriented pyrolytic graphite (HOPG) surfaces using *in situ* STM to monitor the adsorption and aggregation phenomena.

2. Experimental Sections

2.1. DNA Sample Preparation. DNA samples were synthesized and purified by previously reported methods²⁷ and stored in –20 °C freezer before STM imaging.

2.2. STM Samples Preparations and Measurements. Epitaxial Au(111) films on mica used as substrates were prepared using previously described methods.^{29,30} HOPG wafers were purchased from SPI Structure Probe Inc. (West Chester, PA). To prepare a solution of the DNA–chromophore hybrid, trace

* To whom correspondence should be addressed. E-mails: wldeng@scut.edu.cn; dequan@wsu.edu.

[†] South China University of Technology.

[‡] Washington State University.

amount of the solid DNA–chromophore sample was retrieved from the $-20\text{ }^{\circ}\text{C}$ freezer and transferred to an sterilized vial. To the vial containing about 5 grains of the sample were added 5 drops of RNA water and solid dissolved to yield a pink color solution. The above solution was further diluted to almost colorless (faint pink) in another sterilized vial with RNA water.

Subsequently, the sample was sealed and heated gradually from 20 to $80\text{ }^{\circ}\text{C}$ and stayed at $80\text{ }^{\circ}\text{C}$ for 10 min for complete melting of DNA, then cooled very slowly to room temperature. This process usually took a couple of hours and the annealed samples was not disturbed until STM imaging. STM samples were prepared by depositing the above solution dropwise on freshly prepared Au(111) and HOPG substrates. The Au(111) and HOPG substrates with liquid samples on surfaces were then covered with clean glass beakers to allow clean evaporation of water from the surfaces. The prepared samples were ready for STM measurements, and light tracks on the Au(111) and HOPG surfaces could be observed. Each solution sample was used in the heating and cooling cycles for maximum 4–5 times and solution was then disposed.

STM measurements were performed on a Digital Instruments NanoScope IIIa (Santa Barbara CA) scanning tunneling microscope. Both etched W and cut Pt–Ir tips were used. Constant current images were reported.

3. Results and Discussion

Li and co-workers have previously reported a class of oligomers, consisting of rigid chromophores linked by flexible ethylene glycols.³¹ The general strategy is to use a building block, with one end activated and the other end-protected, to attack a chemically reactive group at the growing polymeric chain end. In this way, they have first prepared specific oligomers containing chromophoric dimer, trimer, tetramer, pentamer, hexamer, etc. Further developing this strategy, they have synthesized DNA–chromophore nanostructures by integration of natural and synthetic oligomeric sequences into a single macromolecule and demonstrated that the DNA possessed unusual hyperthermophilic properties.²⁷ In the chromophoric pentamer, π -stack was surrounded by DNA hairpin structures that could be unfolded through binding to the complementary DNA. This chromophoric pentamer surrounded by DNA hairpins has remarkable characteristics on outline motif, topographical shape, and geometrical size, which attract our interests to use STM to further investigate its structural property.

Thin Au(111) films with approximate 150 nm thickness had well-defined terraces and atomic steps and a mean single grain diameter of about 500 nm (Figure 1a). Unlike true single-crystal gold these small crystal showed reconstruction line spacing ranging from 6.3 to $\sim 9.0\text{ nm}$.^{29,30} As a control experiment, we showed here the high resolution atomic STM images of reconstructed Au(111) film in Figure 1. Single atomic steps and reconstruction lines were observed and shown in Figure 1b. High-resolution atomic image (Figure 1c) of Au(111) showed the nearest distance between gold atoms is 0.287 nm which is in excellent agreement with the crystallographical value of $0.288 \pm 0.003\text{ nm}$.

By using STM at different applied potentials, researchers can directly interrogate the electronic properties of DNA as a function of duplex orientation, and can indirectly obtain information about the electronic states of DNA down the helical axis. Because the tunneling current is proportional to the local density of states (LDOS) in the sample,³² images collected at constant current do not necessarily provide the topographical morphology of the surface, but rather important insight into the

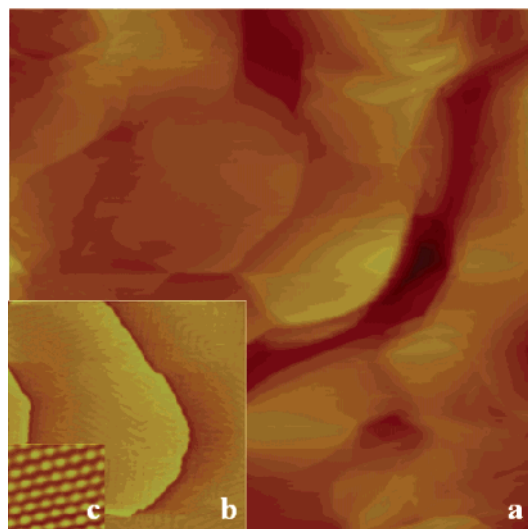


Figure 1. STM images of Au(111) film (a), single atomic steps (b), and gold atoms (c) on mica. (a) Bias voltage is 1.00 V, current is 0.30 nA, and scan size is $1.0 \times 1.0\text{ }\mu\text{m}^2$; (b) bias voltage is 0.70 V, current is 0.30 nA, and scan size is $200.0 \times 200.0\text{ nm}^2$; (c) bias voltage is 0.08 V, current is 1.40 nA, and scan size is $2.0 \times 2.0\text{ nm}^2$.

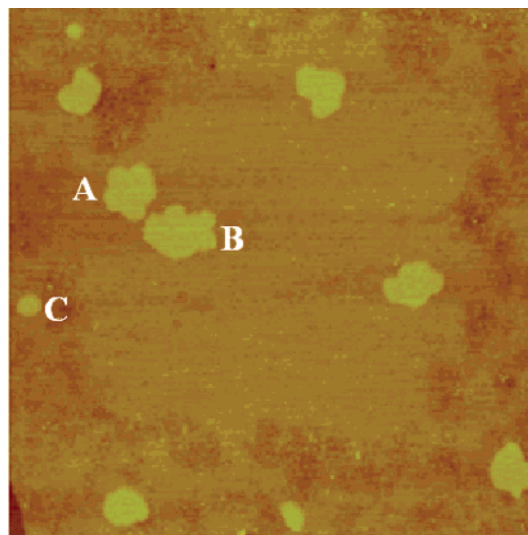


Figure 2. STM image of DNA aggregations on Au(111) surface, bias voltage is 0.80 V, current is 0.30 nA, and scan size is $300.0 \times 300.0\text{ nm}^2$.

LDOS of the DNA.⁹ STM images of DNA agglomerates have also been seen previously.^{33–35} Surfaces containing duplex DNA show features in STM that are most simply explained by the molecules lying approximately flat and with alignment within the DNA film resulting in the formation of domains.³³ Another investigation found that STM images of double-stranded DNA changed with the applied potential; the results seemed to suggest electrostatic interactions between negatively charged DNA helices and the gold surface.³⁴ Overlaps of π -orbitals in DNA bases are no longer efficiently coupled and any conductivity through DNA “wire” is turned off.⁹

Experimentally we found that the DNA–chromophore hybrid molecules form aggregations on Au(111) surface easily. Figure 2 showed the typical aggregations fabricated at ambient conditions, in which the aggregations appeared in different sizes and shapes such as five-lobe flower (A), unregular shape (B), ellipsoid (C), and so on. While dropping solution onto Au(111) substrate, DNA–chromophore molecules adsorbed on the surface in the process of solvent evaporation; concomitantly,

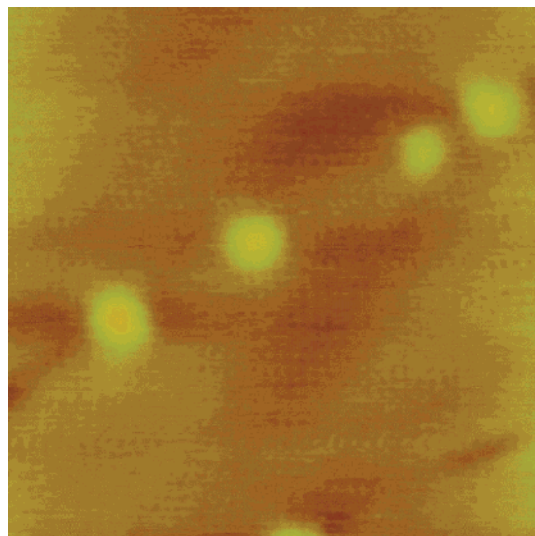


Figure 3. STM image of DNA molecules on HOPG surface, bias voltage is -0.50 V, current is 0.30 nA, and scan size is 100.0×100.0 nm².

aggregation process also started with increasing concentration and solvent evaporation. During the process of adsorption, DNA molecules self-assembled into multimolecule aggregates and the interplay between molecule-substrate and molecule-molecule governed the shape and size of aggregation. These interactions are the driving force for aggregates formation. Between the two major interactions, intermolecular interaction plays a main role in molecular assembly and controls dimension and shape of the aggregation. Unlike chain molecules, the DNA-chromophore hybrid molecules have four-lobe and a cross-like structure, when they adsorbed on Au(111) surface, aggregations grew mostly in two dimensions in various shapes and sizes. This feature is obviously different from those previously reported on DNA molecules.^{9,33,34,36-40}

In Figure 2, within an area of 300×300 nm², there are in total ten aggregates, each with a different topographical shape and geometrical size. For large aggregation, the number of molecule inside is difficult to estimate accurately. However, for small aggregation, one can approximately estimate the number of molecule by measuring the size and by judging the outline of aggregation. Usually, One can only estimate the number ranging from two to four. If the number is over four, the estimation becomes more difficult. For most aggregations in our experiments, height value measured from STM images is nearly constant, ~ 0.30 nm, which provides supporting evidence that DNA-chromophore aggregations grow in two dimensions. In aggregations, molecules arranged close no boundary was observed between molecules.

The same DNA-chromophore hybrid molecules showed a completely different motif while dried on the surface of cleaved HOPG substrate; a typical STM image is shown in Figure 3. Unlike on Au(111) surfaces, DNA-chromophore hybrids adsorbed on the surface mostly as single molecules; their shapes were round and their edges between the molecule and the substrate were indistinct. Moreover, the image resolution was relatively low. These are the major differences between STM images observed on the HOPG substrate and those on the Au-(111) surface. Taking these differences into consideration, we proposed the following hypotheses. First, the interaction between DNA and gold surfaces is stronger than that of DNA and graphite surfaces because of multiple weak interactions between DNA phosphate groups and surface bound metal atoms. Therefore, DNA macromolecules were anchored on gold surface

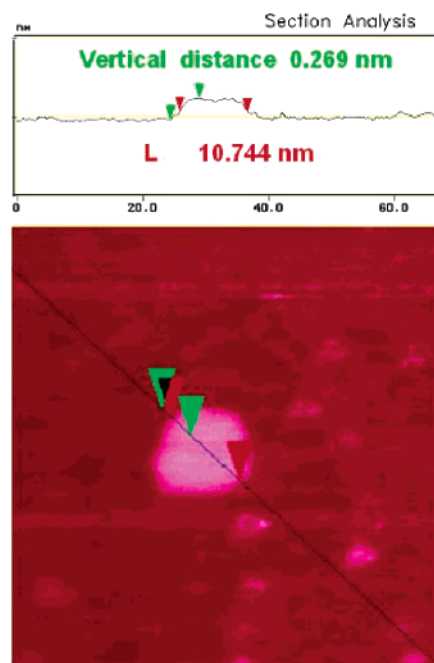


Figure 4. STM image of single DNA molecule on Au(111) surface (down) and sectional profile (up), bias voltage is 0.60 V, current is 0.25 nA, and scan size is 50.0×50.0 nm².

with relatively stronger forces and formed aggregations more firmly immobilized on surfaces. Second, both electronic effect and conductivity should enhance the quality STM images of the aggregates on gold surfaces. Third, since DNA-gold has stronger interactions, DNA-chromophore aggregates adsorbed on gold surfaces remained relatively fixed and does not move easily with the STM tip; this leads to clear boundary between aggregation and gold surface and sharper images. In the HOPG case, since DNA is not "metallic", it is expected that the corrugation of the STM will be reduced when scanning over this macromolecule. The orientation of the cross-shape DNA-chromophore hybrid molecule contrasts previous studies of large DNA fragments⁴¹⁻⁴³ in which the DNA was proposed to order with the helix axis parallel to linear defects on substrates.³⁷ We believe that the nonparallel orientation also feasible for shorter DNA sequences.

In our STM experiments, we also found the DNA-chromophore molecules adsorbed on gold surface as single molecule (Figure 4) as well as smaller self-organized dimer, trimer, and tetramer (Figure 5). For the single molecule, it was immobilized on Au(111) surface, which provided higher resolution STM images. In the single molecule image shown in Figure 4, the motif looks like a four-lobe flower. The lobe is a little bite brighter than the core region; the boundary between lobe and lobe is not well resolved. The cross-sectional profile indicated by a line on this image is also shown in Figure 4. The length of DNA-chromophore pattern from border to border is 10.74 nm, which is in good agreement with the expected length of 10 nm.²⁷ However, the measured height of the pattern is 0.27 nm, much smaller than the expected height of 2 nm.²⁷ The apparent height difference between the measured and the expected is mainly due to the electron effect in the STM scanning and the compact character of the DNA molecule.³⁴ Ellipsometry was used to determine an equivalent thickness of a HS-ssDNA film on gold. In calculating thickness values, a simple model is assumed with uniform film thickness and refractive index of 1.45 . When the DNA 25-mer molecules were adsorbed on the gold through the thiol functionality and stretched to full length, Herne and Tarlov

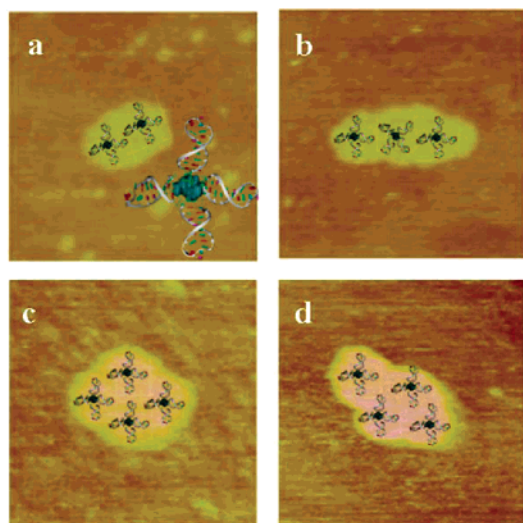


Figure 5. STM images of DNA dimer (a), trimer (b), and tetramers (c, d) on Au(111) surfaces in scan size of $50.0 \times 50.0 \text{ nm}^2$. Overlays are the cross-shape DNA–chromophore hybrid macromolecules in possible orientations and are scaled to the STM images. (a) Bias voltage is 0.65 V and current is 0.20 nA; (b) bias voltage is 0.60 V and current is 0.20 nA; (c) bias voltage is 1.00 V and current is 0.30 nA; (d) bias voltage is 0.60 V and current is 0.50 nA. Inset at low right corner of (a) is the same cross-shape molecule used for the overlays with the STM images.

expected an equivalent film thickness of greater than 16 nm,⁴⁴ approximately 5 times the measured value.³⁸ Because the ellipsometric data give the HS-ssDNA film thickness of approximately 20% of the expected maximum thickness, they conclude that the HS-ssDNA monolayer is not a tightly packed monolayer, and that the DNA chains are not oriented perpendicular to the surface.⁴⁴ For the length and height of the cross-shaped DNA–chromophore hybrid molecule, we also used atomic force microscope (AFM) in the measurements. The length is 10.83 nm, in agreement with the STM measured value, and the height is 0.55 nm, double of the STM measured value. This value is smaller than the expected height, which is typical for AFM measurements on biological samples.

Figure 5a–d showed STM images of dimer, trimer, and tetramer of cross-shape DNA–chromophore on Au(111) surface respectively. Two molecules formed a linear dimer shown in Figure 5a and three molecules formed a linear tetramer shown in Figure 5b. However, different morphology could also form, for example, four molecules self-organized into tetramers with different topographical shapes are shown in Figure 5c and d. The cross-shape DNA–chromophore structures are overlaid on top of the STM images, respectively, corresponding to dimer, trimer, and tetramers with the aggregate sizes matching to the images. In Figure 5c, four DNA–chromophore molecules self-organized into a diamond shape tetramer. Again, no boundary or interface is observed between molecules. In Figure 5d, STM image suggested that four molecules formed an alternated tetramer, which had the shape of an arrowhead. When the number of molecules in an aggregate is greater than four, it is difficult to determine the exact number of molecules in the aggregates with the image topography being more complex. It would be difficult to explain these data without consideration of the contribution of the LDOS of the DNA to the electronic communication from the gold surface to the STM tip. If one takes the orientation of the DNA with respect to the STM tip into consideration, effective orbital overlap between DNA base pairs and the metal electronic states is likely when the DNA is in the upright position with π -plan parallel to the metal surface.

In this orientation, an efficient tunneling process through the energy gap between tip and DNA can occur.⁹ To understand fully the process and mechanism of aggregation of DNA, detail theoretical works are obviously needed, which is one of the future direction of molecular imaging.

As early as 1982, Seeman first proposed using branched DNA building blocks to construct ordered arrays.⁴⁵ Since then, great progresses have been made in two major aspects on nucleic acid-based nanotechnology: production of complex superstructures from simple molecular building blocks, and performance of controlled mechanical movements in molecular devices.⁴⁶ The two studies on a DNA device and a rationally designed RNA building blocks as jigsaw puzzle pieces,^{47,48} demonstrate that it is feasible to build functional materials and devices from “designer” nucleic acids. Active molecular electronic devices include single-molecule transistors and molecular switch tunnel junctions. The development of these more complex devices has been guided by experiment rather than theory.⁴⁹ Up to date, only a couple of systems have passed scientific scrutiny from multiple laboratories. To validate such devices, one compelling approach has been to identify unique properties that can be observed and quantified in both devices and solutions.^{50–53} Various devices made from nucleic acids, including DNA tweezers,⁵⁴ DNA actuator,⁵⁵ DNA bipedal walking machine⁵⁶ and other shape-shifting DNA devices,^{57,58} and RNA molecular jigsaw,⁴⁸ have been reported. In summary, integration of natural and synthetic oligomeric sequences into a single macromolecule provides a fresh new approach to DNA nanostructures and STM or/and AFM are powerful tools for investigating nanostructures and their properties. Fabrication of DNA–based nanodevices is an attractive area, which should receive considerable attention and experience continuous growth.

4. Conclusion

The integration of natural and synthetic oligomeric sequences into a single macromolecule creates foldable DNA–chromophore hybrid nanostructures with unusual thermophilic properties. Scanning tunneling microscope (STM) has been used to further investigate the biological and synthetic nanostructures adsorbed on Au(111) and highly oriented pyrolytic graphite (HOPG) surfaces in ambient conditions. STM investigations suggested the DNA–chromophore hybrid molecules usually formed various aggregations with different geometrical size and topographical shape on gold surface. The DNA–chromophore monomer, dimer, trimer, and tetramer on Au(111) have also been observed. On HOPG surfaces, however, DNA–chromophore hybrid molecules do not form aggregation and exist as adsorbed single molecules. Further analysis of the experimental results indicated interactions between molecule–substrate and molecule–molecule were dominant forces in directing molecular self-organization, which in turn controlled the geometrical sizes and topographical shapes of the aggregations.

Acknowledgment. This work was supported financially by the National Natural Science Foundation of China (20643001), the Scientific Research Foundation for the Returned Overseas Chinese Scholars, State Education Ministry (B09-B7060040), and the Excellent Scientist Program of South China University of Technology (324-D60090).

References and Notes

- (1) Binnig, G.; Rohrer, H.; Gerber, C.; Wicbcl, E. *Phys. Rev. Lett.* **1982**, *49*, 57.
- (2) Binnig, G.; Rohrer, H. In *Trends in Physics*; Janta, J., Pantofliceck, J., Ed.; European Physical Society: The Hague, 1984; p 38.

- (3) Okamoto, A.; Tanaka, K.; Saito, I. *J. Am. Chem. Soc.* **2003**, *125*, 5066.
- (4) Fink, H. W.; Schonenberger, C. *Nature* **1999**, *398*, 407.
- (5) Porath, D.; Bezryadin, A.; de Vries, S.; Dekker, C. *Nature* **2000**, *403*, 635.
- (6) Kasumov, A. Y.; Kociak, M.; Gueron, S.; Reulet, B.; Volkov, V. T.; Klinov, D. V.; Bouchiat, H. *Science* **2001**, *291*, 280.
- (7) Ratner, M. A.; Davis, B.; Kemp, M.; Mujica, V.; Roitberg, A.; Yaliraki, S. In *Molecular Electronics: Science and Technology*; Aviram, A., Ratner, M. A., Eds.; New York Academy of Science: New York, 1998; Vol. 852, p 22.
- (8) Seminario, J. M.; Zacarias, A. G.; Tour, J. M. *J. Am. Chem. Soc.* **2000**, *122*, 3015.
- (9) Ceres, D. M.; Barton, J. K. *J. Am. Chem. Soc.* **2003**, *125*, 14964.
- (10) Seeman, N. C. *Nature* **2003**, *421*, 427.
- (11) Winfree, E.; Liu, F. R.; Wenzler, L. A.; Seeman, N. C. *Nature* **1998**, *394*, 539.
- (12) Malo, J. et al. *Angew. Chem., Int. Ed.* **2005**, *44*, 3057.
- (13) Yan, H.; Park, S. H.; Finkelstein, G.; Reif, J. H.; LaBean, T. H. *Science* **2003**, *301*, 1882.
- (14) Chen, J. H.; Seeman, N. C. *Nature* **1991**, *350*, 631.
- (15) Zhang, Y. W.; Seeman, N. C. *J. Am. Chem. Soc.* **1994**, *116*, 1661.
- (16) Shih, W. M.; Quispe, J. D.; Joyce, G. F. *Nature* **2004**, *427*, 618.
- (17) Dorenbeck, A. *Thesis*, Ruhr-Universitat Bochum **2000**.
- (18) Scheffler, M.; Dorenbeck, A.; Jordan, S.; Wustefeld, M.; Kiedrowski, G. V. *Angew. Chem., Int. Ed.* **1999**, *38*, 3312.
- (19) Goodman, R. P.; Schaap, I. A. T.; Tardin, C. F.; Erben, C. M.; Berry, R. M.; Schmidt, C. F.; Turberfield, A. J. *Science* **2005**, *310*, 1661.
- (20) Elghanian, R.; Storhoff, J. J.; Mucic, R. C.; Letsinger, R. L.; Mirkin, C. A. *Science* **1997**, *277*, 1078.
- (21) Mitchell, G. P.; Mirkin, C. A.; Letsinger, R. L. *J. Am. Chem. Soc.* **1999**, *121*, 8122.
- (22) Maxwell, D. J.; Taylor, J. R.; Nie, S. M. *J. Am. Chem. Soc.* **2002**, *124*, 9606.
- (23) Saghatelian, A.; Guckian, K. M.; Thayer, D. A.; Ghadiri, M. R. *J. Am. Chem. Soc.* **2003**, *125*, 344.
- (24) Waybright, S. M.; Singleton, C. P.; Wachter, K.; Murphy, C. J.; Bunz, U. H. F. *J. Am. Chem. Soc.* **2001**, *123*, 1828.
- (25) Ren, R. X. F.; Chaudhuri, N. C.; Paris, P. L.; Rumney, S.; Kool, E. T. *J. Am. Chem. Soc.* **1996**, *118*, 7671.
- (26) Bevers, S.; O'Dea, T. P.; McLaughlin, L. W. *J. Am. Chem. Soc.* **1998**, *120*, 11004.
- (27) Wang, W.; Wan, W.; Zhou, H. H.; Niu, S.; Li, A. D. Q. *J. Am. Chem. Soc.* **2003**, *125*, 5248.
- (28) Gait, M. J. *Oligonucleotide Synthesis: A Practical Approach*; IRL Press: Washington, DC, 1984.
- (29) Deng, W.; Hipps, K. W. *J. Phys. Chem. B* **2003**, *107*, 10736.
- (30) Lu, X.; Hipps, K. W. *J. Phys. Chem. B* **1997**, *101*, 5391.
- (31) Wang, W.; Li, L. S.; Helms, G.; Zhou, H. H.; Li, A. D. Q. *J. Am. Chem. Soc.* **2003**, *125*, 1120.
- (32) Tersoff, J.; Hamann, D. R. *Phys. Rev. B* **1985**, *31*, 805.
- (33) Patole, S. N.; Pike, A. R.; Connolly, B. A.; Horrocks, B. R.; Houlton, A. *Langmuir* **2003**, *19*, 5457.
- (34) Zhang, Z. L.; Pang, D. W.; Zhang, R. Y.; Yan, J. W.; Mao, B. W.; Qi, Y. *Bioconjugate Chem.* **2002**, *13*, 104.
- (35) Li, B.; Zeng, C. G.; Li, Q. X.; Wang, B.; Yuan, L. F.; Wang, H. Q.; Yang, J. L.; Hou, J. G.; Zhu, Q. S. *J. Phys. Chem. B* **2003**, *107*, 972.
- (36) Lindsay, S. M.; Thundat, T.; Nagahara, L.; Knipping, U.; Rill, R. L. *Science* **1989**, *244*, 1063.
- (37) Kim, Y.; Long, E. C.; Barton, J. K.; Lieber, C. M. *Langmuir* **1992**, *8*, 496.
- (38) Herne, T. M.; Tarlov, M. J. *J. Am. Chem. Soc.* **1997**, *119*, 8916.
- (39) Yang, M. S.; Yau, H. C. M.; Chan, H. L. *Langmuir* **1998**, *14*, 6121.
- (40) O'Brien, J. C.; Stickney, J. T.; Porter, M. D. *J. Am. Chem. Soc.* **2000**, *122*, 5004.
- (41) Lee, G.; Arscott, P. G.; Bloomfield, V. A.; Evans, D. F. *Science* **1989**, *243*, 1708.
- (42) Arscott, P. G.; Lee, G.; Bloomfield, V. A.; Evans, D. F. *Nature* **1989**, *339*, 484.
- (43) Keller, D.; Bustamante, C.; Keller, R. W. *Proc. Natl. Acad. Sci. U.S.A.* **1989**, *86*, 5356.
- (44) Peterlinz, K. A.; Georgiadis, R. M.; Herne, T. M.; Tarlov, J. M. *J. Am. Chem. Soc.* **1997**, *119*, 3401.
- (45) Seeman, N. C. *J. Theor. Biol.* **1982**, *99*, 237.
- (46) Yan, H. *Science* **2004**, *306*, 2048.
- (47) Liao, S.; Seeman, N. C. *Science* **2004**, *306*, 2072.
- (48) Chworos, A.; Severcan, I.; Koyfman, A. Y.; Weinkam, P.; Oroudjev, E.; Hansma, H. G.; Jaeger, L. *Science* **2004**, *306*, 2068.
- (49) Flood, A. H.; Stoddart, J. F.; Steuerman, D. W.; Herth, J. R. *Science* **2004**, *306*, 2055.
- (50) Metzger, R. M. *Chem. Rev.* **2003**, *103*, 3803.
- (51) Ashwell, G. J.; Tyrrell, W. D.; Whittam, A. J.; *J. Am. Chem. Soc.* **2004**, *126*, 7102.
- (52) Liang, W.; Shores, M. P.; Bockrath, M.; Long, J. R.; Park, H. *Nature* **2002**, *417*, 725.
- (53) Katz, E.; Lioubashevski, O.; Willner, I. *J. Am. Chem. Soc.* **2004**, *126*, 15520.
- (54) Yurke, B.; Turberfield, A. J.; Mills, A. P., Jr.; Simmel, F. C.; Neumann, J. L. *Nature* **2000**, *406*, 605.
- (55) Simmel, F. C.; Yurke, B. *Phys. Rev. E* **2001**, *63*, 041913.
- (56) Sherman, W. B.; Seeman, N. C. *Nano Lett.* **2004**, *4*, 1203.
- (57) Mao, C.; Sun, W.; Shen, Z.; Seeman, N. C. *Nature* **1999**, *397*, 144.
- (58) Yan, H.; Zhang, X.; Shen, Z.; Seeman, N. C. *Nature* **2002**, *415*, 62.